Demonstration of Autonomous Sampling Techniques in an Icy Moon Terrestrial Analog

Joseph Bowkett, David Inkyu Kim, Jeremy Nash, Daniel Pastor Moreno, Matt Gildner, Rohan Thakker, Kris Wehage, Sung-Kyun Kim, Alex Brinkman, Blair Emanuel, Jeffrey Edlund, Barry Ridge, Abhi Jain, and Paul Backes
NASA Jet Propulsion Laboratory
California Institute of Technology
bowkett@jpl.nasa.gov

***Abstract*—A collection of functional autonomy behaviors to allow unsupervised science sample selection and collection on Icy Moons such as Europa or Enceladus was demonstrated on the terrestrial analog of Matanuska Glacier, AK, USA. Candidate sample sites are autonomously identified within the workspace, assessed for feasibility of successful collection, and surface material excavated while both preventing and responding to tool faults arising during interaction with the environment. A description of the system and lessons learned from the field application are discussed with respect to how they may impact potential future surface sampling missions to Icy Moons.**

TABLE OF CONTENTS

1. INTRODUCTION

The icy moons of the solar system, in particular Europa and Enceladus, have been the focus of significant scientific interest in recent decades due to their potential to harbour liquid water conducive to life as we know it [1], [2]. By 2012, images from the Hubble Space Telescope of Europa's south pole supplied plausible evidence of water plumes ejecting from the surface [3], [4], thus motivating planetary science to pursue exploring the possibility that subsurface oceans could support life. Similar plumes were observed over Saturn's moon Enceladus in 2006 during a Cassini flyby [5]. It has been theorized that organic molecules from the subsurface oceans could, if present, be ejected onto the surface of Europa and be suitable for biosignature detection; if preserved under 10-20cm of surface material as protection from the extreme Jovian radiation [6]. This motivates being able to excavate between 10 and 30cm below the surface before collecting samples for analysis [7], so as to improve the chance of bioginatures being detectable.

This surge in interest in exploration of icy moons led to the proposal of a NASA/JPL Europa Lander mission [8], [9] to conduct surface sampling and attempt to identify organic molecules or "biosignatures" that might have been ejected from subsurface oceans by these observable plumes. Recent efforts have included the development of autonomous sampling capabilities [10], planning and executive mission layers [11], and deep space Ground-in-the-Loop concepts [12], a subset of which was recently demonstrated in the the Jet Propulsion Laboratory's (JPL) Europa Lander Field Sampling Campaign (ELFS Camp) at Matanuska Glacier, Alaska, USA in July and August of 2022. The first deployment site can be seen in Fig. 1. 58 tests were conducted over the course of the 3 week trial.

The technology developments efforts above were guided by a reference mission concept that involved robotically accessing subsurface material 10cm - 30cm beneath the Europan surface through excavation, collecting sample at that depth, and transferring the sample into instrument system on the lander. This paper focuses on the excavation and collection aspects of the sampling problem.

Figure 1: The Europa Lander Field Sampling Campaign (ELFS Camp) system at sampling site A on Matanuska Glacier, AK. Four passively adjustable legs stabilize a central base, atop of which a pan-tilt unit affords pointing of a perception head comprised of a stereo camera pair and LED illuminator. The 5 DoF "Luigi" arm and ICEPIC drilling/sampling tool are seen engaging the ice, while power and compute tethers connect to Ground Support Equipment (GSE) out of view to the right.

978-1-6654-9032-0/23/$31.00 ©2023 IEEE

While many of the sampling behaviors and mission activities could be simulated within a laboratory environment, it was anticipated that there were many additional challenges to be found operating in a terrestrial analog of an icy moon. Due to this, baseline behaviors were developed within a laboratory setting, capturing all off-nominal scenarios that could be conceived of therein, and then a field trial used to elucidate the additional challenges. These ended up including stability considerations, ease of re-engaging past excavations, difficulties in perceiving surrounding terrain in daylight conditions, and the changing of surrounding topography due to surface melting during operations; all of which are detailed and the final sections of this paper.

In preparation for the Alaska field campaign, an operational readiness test (ORT) was conducted within the Jet Propulsion Laboratory's 'Mars Yard' in April of 2022. This served to qualify the ground support equipment that had been fabricated to operate the electromechanical systems in the field away from mains power supply, as well as exercise the team's ability to source outside corrective input from other staff members while on deployment. The same sequence of baseline and reach demonstrations planned for the field campaign were exercised in this venue to ensure that operating procedures were sufficiently documented to allow rapid deployment in-situ. However, 'reach', or the most unlikely to succeed goals were left for final testing at the field campaign sites within Matanuska Glacier, AK.

2. STRUCTURE

Section 3 describes the physical sampling system upon which the autonomy system operates, both within lab testbeds and the extended system deployed to the field. Section 4 then depicts the structure of the assembled autonomy system, including both "planning & execution", "functional" sampling, and perception autonomy. Sections 5 and 6 go on to explain the functionally autonomous perception of the workspace environment and the sampling behaviors that interact with it respectively. Section 8 describes the results of field campaign effort. Section 9 provides a list of lesson learned during the field campaign. Lastly, section 10 proposes some future areas of technical development that could both explore and address the challenges from the prior section.

3. SAMPLING SYSTEM

The lander sampling system consists of one of two serial rotary robotic arms of varying degrees of freedom (DoFs) equipped with manually interchangeable sampling tools, with visual inspection of the environment and tools afforded by a "perception head" consisting of a stereo pair of Baumer RGB cameras atop a pan-tilt unit. These systems are deployed on a lander mock-up made up of a central extruded aluminum frame, a gripping belly pan, and four 2-DoF articulated legs capable of manual lockout. The lander mock-up was designed to represent the basic dimensions of a conceptual Europa lander and provide a passive stabilization system able to react sampling loads into the terrain and reduce slip in terrestrial environments. Pictured in Fig. 1 is the full system as deployed in the both the ORT and the early stages of the field trial with Luigi arm and ICEPIC tool.

Robotic Arms

There were two models of robotic arm present during both laboratory development and field testing of the sampling autonomy system. The robotic arms are referred to as the Luigi arm and RiNG arm. Key differences between the Luigi and RiNG arms respectively included reach (1.4m vs 2.1m), the number of degrees of freedom (5 vs. 7), the cable routing through the electromechanical system (external vs internal) and the magnitude of force that could be applied in the tool frame (350N vs 500N). Both arms were equipped with manual tool changers to facilitate rapid reconfiguration of the arms for different sampling autonomy development activities. The majority of sampling behaviors were developed with the kinematic constraints of the five degree of freedom Luigi arm in mind such that the additional degrees of freedom off the RiNG arm were under-utilised for portions of the field campaign.

Luigi Arm—The Luigi arm is a 5 degree of freedom system in a yaw pitch pitch pitch yaw (YPPPY) configuration, as seen in Fig. 2. It is equipped with an end effector-mounted ATI Delta IP68 force torque sensor with a sensing capacity of 600N and 60Nm. This arm was inherited from a Mars Curiosity mission testbed and mimics the 5-DoF configuration common to arms flown on Mars missions, where the underactuated nature of the system limits the ability of the tool to achieve arbitrary orientation within the workspace. Such a limitation can be handled by placing geometric constraints on the sampling targets selected for excavation within the workspace (described in Sec. 5) such that tool tip trajectories remain within what is termed the "sagittal" plane, or the plane normal to the range of motion with joints 2, 3, and 4 for a given yaw angle of joint 1 (co-planar with the page in the CAD model configuration depicted Fig. 2). In the case of using a rotary tool such as ICEPIC (seen below), which only requires 5 dimensions of position to engage a given point, this simply constrained the range of approaches angles that could realized on an arbitrary geometry within the workspace.

For a scoop, however, which requires full 6-DoF positioning to realize arbitrary tool motions, this constraint proves more restrictive and collapses the "fully manipulable" space for the tool onto the SE(2) sagittal plane. While motions outside this plane are possible, they are non-holonomic in nature and thus more challenging to plan, such that scooping behaviors with the Luigi arm were artificially constrained to operate along the sagittal plane afforded by a given joint 1 yaw angle, moving material radially towards or away from the lander base.

RiNG Arm—The ReconfIgurable Next Generation (RiNG) arm is a new 7-DoF robotic arm developed at JPL that uses internal distributed motor control and harnessing, allowing weatherproofing for operation in challenging environments, such as glaciers, and enhanced robustness to icy sampling. It uses a yaw pitch roll pitch roll pitch yaw (YPRPRPY) configuration. It is equipped with an end effector-mounted ATI Omega85 IP68 force torque sensor with a sensing capacity of 2000N and 100Nm. Along with affording additional degrees of freedom, the RiNG arm also achieves a greater total reach than that of the Luigi arm (achieving max 2.1m from the arm base) and multi-turn joint range of motion, such that both the reachability across the sampling workspace, and the volume of the workspace are increased. The use of high torque density custom actuators made up of outrunner motors and 160:1 harmonic gears enables a payload of 10kg with the ability to apply a 500N sampling across the reachable workspace.

While the RiNG arm facilitated drilling with the ICEPIC tool at greater normal forces than the Luigi arm, the primary

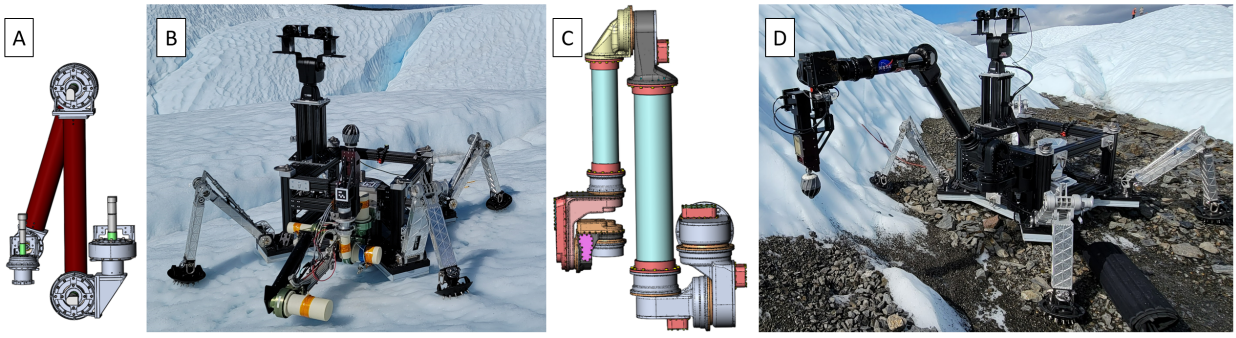

Figure 2: A) The Luigi 5-DoF arm CAD model, in Yaw Pitch Pitch Pitch Yaw configuration. The underactuated system imposed geometric constraints on the orientations achievable with a given end effector. B) The Luigi arm mounted on the lander mockup in the field. C) The 7-DoF RiNG arm CAD model in Yaw Pitch Roll Pitch Roll Pitch Yaw configuration. This configuration achieves full manipulability across the sampling workspace. D) The RiNG arm mounted on the lander mockup in the field.[10]

advantages were derived during scooping behaviors, which benefited more from the freeing from kinematic constraints. The distribution of the electronics along the arm also allows additional capabilities to be embedded within the weather proofed housings. This included an wrist mounted camera, a RealSense D435i connected to a internal Raspberry Pi 4 single board computer, which allows RGB video and point clouds to be generated and sent back along a network connection to the off-board primary compute system.

Tools

ICEPIC—For the purpose of combined aggressive rotary excavation and collection, a tool was developed under contract with Honeybee Robotics. This tool, termed the Ice Collection and Excavation Primary Integrated Cutter, or ICEPIC, is pictured in Fig. 3. A central commercial-off-the-shelf (COTS) core box router bit is surrounded by 12 custom shaped serrated blades mounted to a hollow hemispherical shell. Both the core box router and surrounding teeth serve to remove material during operation of the excavation mode of the tool.

A collection configuration of the tool is achieved with an addition of a spacer that draws the core box router backwards into the hollow within the hemispherical structure. This configuration forms an open ring into the shell's interior. During cutting, tailings generated by the teeth are lifted and thrown through that opening into the interior of the tool. The spinning of the blade holds the tailings in place inside the shell due to the centrifugal forces acting upon them. In this collection configuration of ICEPIC the material gathered within the internal cavity is retained by keeping the tool spinning until it can be moved over a sample receptacle. Sample can then be transferred out of ICEPIC through gravitational forces or through a pneumatic transfer dock. Gravitational transfer was used for autonomy development and testing.

The ICEPIC blade is spun using a JPL-designed drive with a geared, brushless motor equipped with an incremental position encoder. During cutting operations the output is run between 500-1146 rpm, depending on the properties target sample substrate and feed rate of the arm. Torque output was typically below 1.5Nm when cutting, although the drive is capable of higher outputs as needed.

While the hemispherical shape of ICEPIC was intended to make it robust to a variety of approach angles to the surface of the substrate, it was discovered during lab testing that during lateral cutting motions the tool generated high reaction torques at the tool base that would exceed cross-moment torque sensing capacities of the force torque sensors mounted on the arms. This was a result of tool tip lateral loads acting at a large, 51cm offset from the force torque sensors in the current tool mounting configuration. Due to this phenomenon, plunging type motions with minimal lateral loads were relied upon for excavation and collection purposes.

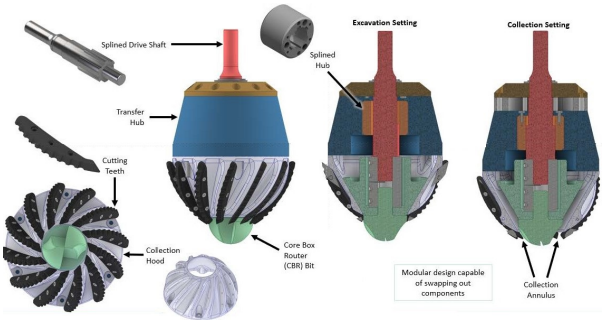

Figure 3: The aggressive excavation and collection tool that was employed by the sampling autonomy during the field trial is named ICEPIC, or Ice Collection and Excavation Primary Integrated Cutter. By adjusting a spacer within the internal structure, the central core box router bit can be extended for pure excavation, or retracted to allow material to accumulate inside an internal cavity, thus enabling sample collection.

Scoop—Two generations of scooping tools were developed for the purpose of scraping and scooping unconsolidated surface material away to expose hard substrate underneath. The second generation design, as seen in Fig. 5, was used to develop scooping behaviors on crushed garnet granular material within a laboratory environment with both homogeneous and stratified materials. Of greatest interest was the ability to remove granular material from atop a hard substrate such as ice, so as to expose potential sampling sites for the ICEPIC tool to excavate further.

Early development was conducted on a 5-DoF arm of a similar configuration to Luigi, where motion was constrained to

the sagittal plane. Excavations of loose surface material were effective in a contrived laboratory environment, however, when applied in the significantly more topographically interesting Alaskan glacier, the trajectories of the scoop proved only marginally effective at conforming to the terrain so as to remove most granular media on the thin substrate. Transfer of the script tool to the 7-DoF RiNG arm significantly improved the sampling system's ability to track the surface of the ice substrate with the scoop. During two glacier tests using the scoop mounted on the RiNG arm the system was able to remove the majority of a single layer of 1-6cm loose gravel material atop a icy substrate.

Figure 4: Example scoop interaction with glacier terrain. The top layer is composed of small loose gravel and the lower layer is solid ice. The scoop adapted to the terrain and it removed the top layer to expose the ice beneath for ICEPIC drilling and sampling.

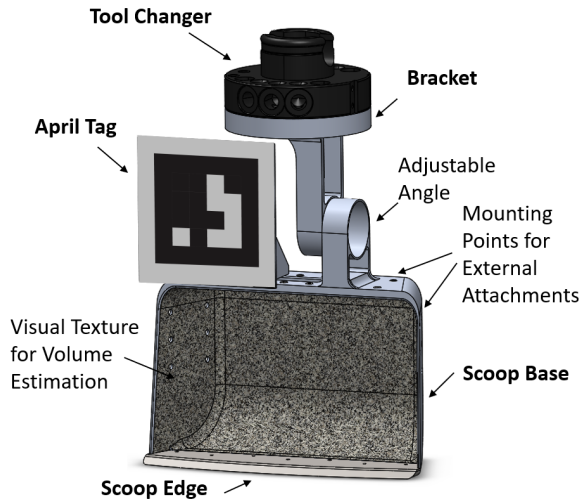

Figure 5: This scoop design is the second iteration developed after earlier test campaigns used a repurposed model from the Mars Phoenix Lander. Improvements include a wider cross-section and back swept rear section to reduce drag and stiction along the sides. A textured pattern allows the perception system to more easily detect the presence of material for volume estimation, while an affixed AprilTag [13] enables visual determination of tool pose for comparison to forward kinematics.

Physics Simulation Environment

Simulation of the lander sampling system, as well as its environment and its interactions with the environment, is provided by SAELSIM - a customized version of DARTS (Dynamics Algorithms for Real-Time Simulation) [14], which is a high-fidelity, flexible multibody dynamics simulator used for real-time hardware-in-the-loop design, integration and testing of spacecraft flight software. The goal of SAELSIM is to simulate the mechanisms and tool-terrain interaction of autonomous sampling using a Luigi arm model attached to the Europa Lander model. This simulated testbed can be used to develop and test autonomous sampling behaviors which modify the 3D workspace using a high DoF manipulation system equipped with force torque and perception feedback. SAELSIM consists of a Europa lander model with mast, cameras, legs, and a 5-DoF Luigi arm with either a saw, scoop or ICEPIC tool attached. The surface of the workspace can be specified by a surface DEM and the material properties of the soil under the surface can be specified. The workspace information is stored as OpenVdDB voxel grids [15]. The tool can also be used to push against and remove material from the workspace. Images captured from SAELSIM are illustrated in Figure 6.

The lander model consists of a main body, mast with attached camera, and 4 independently moving legs. At the start of the simulation the lander is settled so that the bottom plate of the lander is 0.3 meters above the tallest point of the DEM under the lander body by default. The lander's legs are initially limp and bend such that they are in contact with the surface (if possible). After the lander has settled and once its legs have been pinned in place, it will not slip or move in any way. The Luigi arm model is a 5-DoF serial manipulator with a roughly 1.4 meter reach configured in a Yaw - Pitch - Pitch - Pitch - Yaw kinematic layout. The desired joint states are commanded by publishing to a particular ROS topic. Each joint angle is controlled by a DARTS PinDamperAssembly model with a PID controller with proportional coefficient ($kp = 500$), derivative coefficient ($kd = 400$), integral coefficient ($ki = 100$), $max\_torque = 300$, and $damping = 0.1$. Actual joint states, as well as wrist force-torque measurements, are reported back toe the CASAH environment via a set of ROS topics that match those used on hardware; facilitating easy transfer between them.

When it comes to modeling surface material interactions, the terrain surface material is modeled as a topological voxel grid and each tool has a collision mesh and a destructive mesh. The collision mesh is defined by the arm assembly and is used for both visual display and collision detection. Currently the Flexible Collision Library (FCL) [16] is used for detecting collisions with the terrain. The external force applied to the tool from each contact is calculated using a spring damper model. The stiffness and damping parameters for each contact are based on the material type of the terrain at the point of contact. The tool's destructive mesh is smaller than the collision mesh so that if the saw, scoop or ICEPIC tool is pushed into the terrain, material inside the destructive mesh is removed from the terrain. This process is illustrated in Figure 7.

Laboratory Environment

During development of the sampling autonomy, both the Luigi and RiNG arms, with their interchangeable tools, were deployed within an indoor laboratory environment affixed to 8020 framing. An example of the fixturing frame for the RiNG arm can be seen in Fig. 8, alongside a human model for scale. Weights at the back of the fixturing bracket were required to resist the significant moment incurred upon the frame by pressing down with the full strength of each arm. A perception head of the same design that was used within the

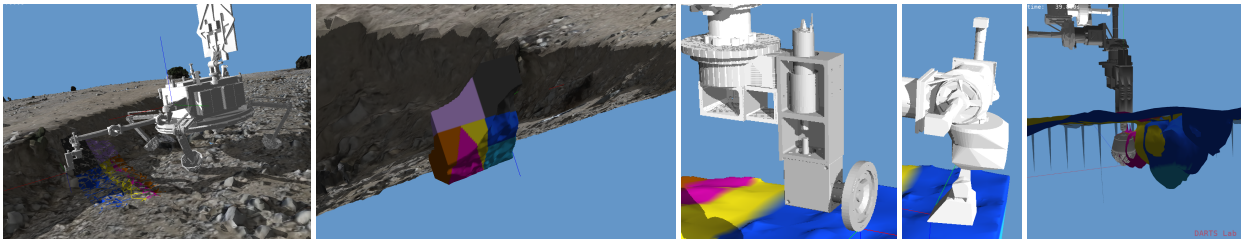

Figure 6: Images captured from SAELSIM. From left to right: the Europa lander model with Luigi arm positioned on a surface model derived from a DEM with accompanying rainbow-colored topological voxel material model; the topological voxel material model as seen from beneath the surface model; the saw tool; the scoop tool; and the ICEPIC tool interacting with the topological voxel material model.

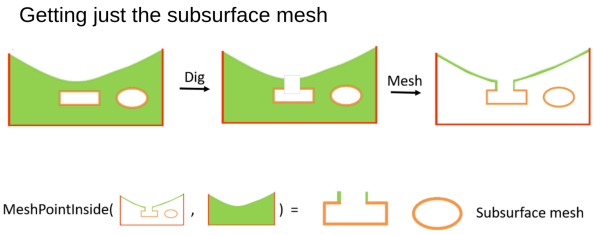

Figure 7: The SAELSIM topological voxel grid terrain material model tool collision and material destruction process.

field deployment could be attached above the arm fixturing frame, affording a complete view of the nominal sampling workspace when each arm was suitably maneuvered out of view.

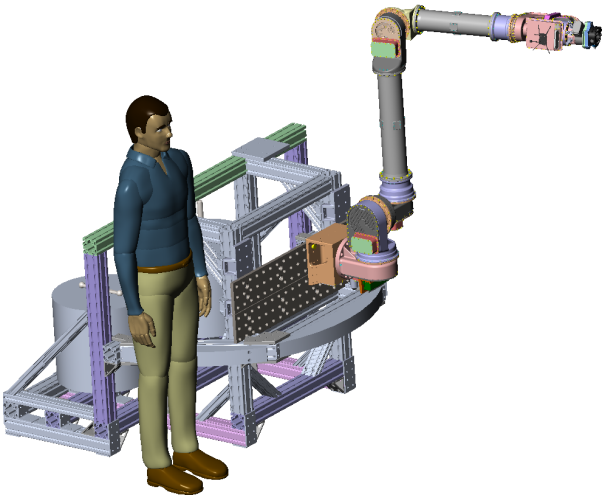

Figure 8: The RiNG arm attached to the 8020 framing that forms the laboratory fixture, alongside a human model for scale. The tool changer may be seen as the black distal element, while the tool camera box can be seen in pink with gray/black Realsense D435i protruding to the right.

Simulants—Ambient simulants were selected for a laboratory environment that would elicit a range of autonomy and tool performance responses. These simulants were not expected to mimic any specific characteristics of the Europan surface given the high uncertainty in Europan surface properties and difficulty in replicating such properties at ambient. Simulants could be placed within the operating workspace of each deployed arm. Granular simulants, including crushed garnet and Mojave Mars Simulant dust [17], were deployed in bins. Consolidated simulants, including wood and machining wax, were affixed in ballasted clamp fixtures or in the case of deionized water ice simulants, secured in 30cm x 48cm x 25cm bins mounted on ballasted LN2-chilled coldplates. The icy simulant fixture developed by JPL's Extraterrestrial Simulants Group is referred to as the Test Article Containment and Transportation System (TACTS).

Lab testing with ambient simulants served well to architect the autonomy system, define sampling behaviors, and develop arm and tool operating setpoints (e.g. preload, feed, speeds). However, the small size of the lab ambient simulants and the impacts of the fixturing systems often limited the ability to test the full adaptability of autonomous sampling behaviors. The lab simulant setup also introduced 'test-isms' that were highly specific to the lab, e.g. needing to highly constrain via software keep-in volumes the site selection algorithm to the small area of the simulant. These were primary reasons for exercising the sampling system in varied set of field environments.

Fig. 9 shows the ICEPIC tool in preparation to engage the surface of an ice sample affixed at a 45° angle with respect to gravity. A depth camera may be seen in the background recording contextual video as well as point clouds of the surface during each stage of drilling. Liquid nitrogen connections may be seen protruding from the base of the TACTS bin.

4. SOFTWARE TOPOLOGY

The software that operates the sampling activities during the Alaska field campaign is comprised of three elements. The first of these and the lowest in the hierarchy is that of the sampling functional autonomy which undertakes individual behaviors in order to realize a specific goal such as excavating to a particular depth or collecting a certain quantity of material. The higher level of pure software capability is described as "mission autonomy", where a planning and executive engine chooses when to expend various mission resources such as time and energy by commanding the functional autonomy to conduct behaviors. Atop this planning and executive layout sits the operator interface, equivalent to a ground in the loop (GitL) connection, where human operators can direct the top level mission goals and assign constraints on resource use by the mission autonomy layer.

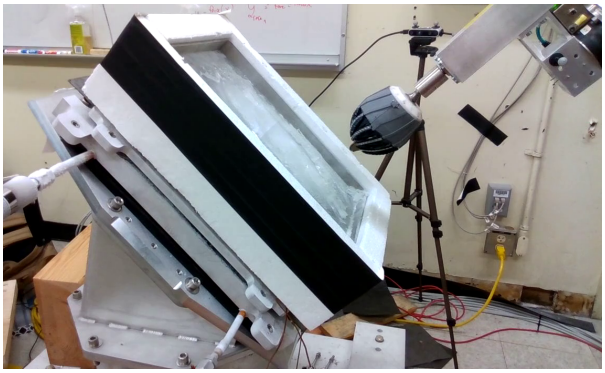

Figure 9: Experiments with de-ionised water ice in a laboratory environment were housed within the Test Article Containment and Transportation System (TACTS), developed by JPL's Extraterrestrial Simulants Group. This fixturing system used liquid nitrogen and thermocouples to regulate subsurface temperature of premade ice samples which were typically maintained at -20C during testing.

The field operations were structured around a baseline set of sampling relevant to a reference mission, with an array of 'reach' goals to extend the demonstrated capabilities beyond those tested within a laboratory environment. For the reference mission the sampling activities consisted of: A) capturing a panoramic image of the surrounding area, B) conducting a visual survey of the reachable sampling workspace, C) identifying and selecting from feasible sampling site candidates within that region, D) excavating the chosen site to the predetermined depth, E) connecting sample and transferring it to a scale repetitively until sufficient mass was achieved. An example of this mission execution can be seen in Fig. 10, where the TRACE mission autonomy framework [18] uses a Business Process Model and Notation (BPMN) to plot out the sequence of activities.

The functional sampling autonomy described within this paper was formulated within the Control Autonomy for Sample Acquisition and Handling (CASAH) environment [19]. The latest version of this environment is built upon a foundation of the ROS1 Noetic code base, using the Ubuntu 20.04 operating system. Interfaces to the motion controllers and force torque sensors that comprise the majority of the proprioceptive system were provided by the FastCAT EtherCAT library [20]. Behaviors were structured in a hierarchical, modular fashion using ROS1 actions, topologically equivalent to hierarchical state machines (HSMs) in order to reduce redundancy and level of validation effort across the compound activities the system was to undertake.

Operator Interface

Fig. 11 demonstrates a capture of the operator interface in use during activities at the second 'landing' site during the field trial. Three context video streams on either side of the screen provide operator cognizance of the actions of the platform, while all features within the central window represent the systems self knowledge and understanding of its immediate environment. The perception system provides a digital elevation model, or DEM, of the sampling workspace, and forward kinematics allow the position and past and future trajectories of the tool to be plotted alongside.

Textual overlays of this window offer insight into the present

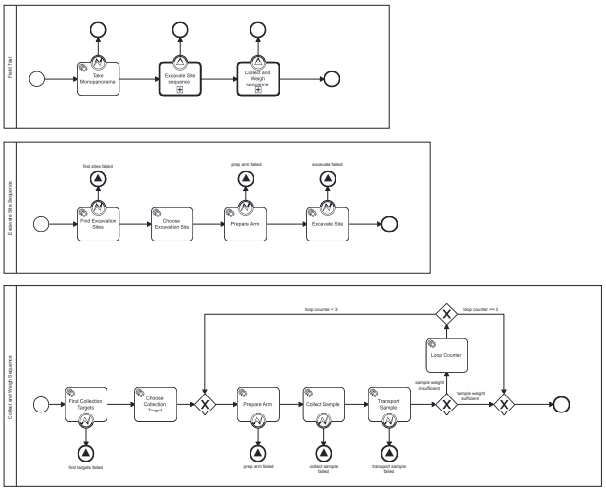

Figure 10: A hierarchical Business Process Model and Notation (BPMN) model for a nominal mission plan executing within the Traceable Robotic Activity Composer and Executive (TRACE) tool. As this is a nominal mission plan, most activities happen sequentially, save that "Collect Sample" will loop up to 3 times until sufficient sample mass is collected.

status of relevant modules and whether or not a test log is actively running. Planned tool trajectories and joint configurations can also be visualized white enabling the relevant visualization channel within the ROS1 RVIZ environment.

5. WORKSPACE PERCEPTION

Exteroceptive sensing of the sampling workspace was provided by a pair of stereo cameras atop a pan-tilt unit (PTU), which allowed them to be aimed at any location within the sampling workspace, and also conduct panoramic imaging for stitching situational mosaic images. Stereo point clouds were generated by local block matching by default, or semi-global matching in texture-poor terrain. The stereo point clouds were aggregated into a digital elevation model (DEM), which captures terrain height across a discrete cm-resolution grid in addition to visual and geometric statistics for identifying candidate sampling sites. Each cell contained an estimate of surface normal and roughness, based on a least-squares plane fit to a local neighborhood of aggregated stereo points, and average color and height. These parameters were packed into a two-dimensional array of objects and transmitted as a ROS message type between the perception and sampling autonomy subsystems for use in planning excavation and collection activities.

Candidate Site Selection

After receiving the augmented DEM from the vision system, a module within the autonomy stack explored regions within the reachable topography to find candidate sampling sites. A hierarchy of constraints was evaluated at each of the inspected candidate points, which would form the origin of a sampling site, including keep-out and keep-in zones, reachability given the constraints of the arm in question, and the volume of the anticipated excavation region. Fig. 12 depicts an abstraction of a candidate sampling site with each of the poses about a sampling volume that are checked for reachability.

Figure 11: Operator interface deployed during Alaska field trial demonstration based on ROS1's RVIZ. Context video streams from a webcam and two RealSense cameras are pictured alongside, the latter of which also provide point clouds for comparison against "on-board" sensing. Other information streams such as forward kinematic model, DEM, historical and planned tool trajectories, and sample targets may be selected from the left panel. Test and system status are overlayed in blue text on the 3D visual panel.

Points within the keep-in zones were subsampled to reduce the computation time and need for complete canvassing. Sampling began from the center of the keep-in zone, or nominal sampling workspace, and extended outwards until sufficient candidates were found, typically a limit of 10. Each time a valid candidate site was found it was added as a new exclusion zone so as to not have sampling regions overlap. Future developments may wish to add dilation to these keep-out regions in an effort to prevent cross contamination of tailings that are generated during aggressive excavation.

Lander Slip Monitor

A capability was developed to continuously monitor lander slip during sampling operations. The design goals were to detect small movements of the lander base while ignoring significant vibrations during sampling operations, report slips with minimal delay (sub-second) to minimize hardware damage, prioritize recall first and precision second, and minimize computational burden. The system used an industrial grade VectorNav VN-100 IMU with an onboard AHRS providing orientation estimates from the gyroscope and accelerometer. With the IMU fixed to the lander base, the lander computer monitored for rotations over a 0.25s window that exceeded a 0.1deg threshold. Lab and field testing demonstrated that the system could detect subtle slip motions even when the lander was significantly vibrating during sampling operations. While no significant slips were detected during field trial operations-other than those intentionally imposed upon the system for verification of the monitor-this slip detection would allow fault monitors within the samplings behaviors to halt operations retract the tool in the case that motion of the base was detected; to reduce risk of damage to the sampling tool and articulated arm.

Perception System Calibration

To provide accurate DEMs in the lander's reference frame, three transforms in the perception system needed to be calibrated: left camera to right camera, left camera to PTU, and PTU to lander. The PTU to lander calibration was estimated by pointing the cameras at an AprilTag fixed to the lander base and minimizing tag corner reprojection error in both left and right cameras to improve accuracy. Left camera to PTU calibration used a dual quaternion based hand-

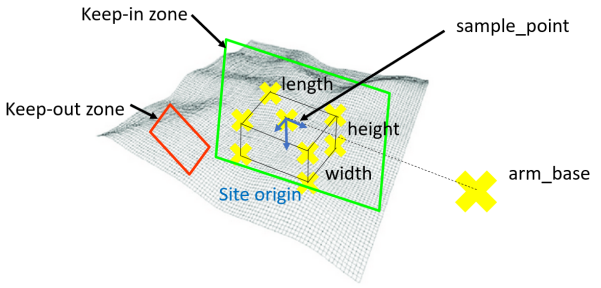

Figure 12: An abstraction of the "sample site selection" pipeline, where the grid represents a Digital Elevation Model (DEM) supplied by the perception system. Red zones are designated "keep-out" such that no candidate site will overlap them, green zones are designated "keep-in" (typically denoting the outer bound of the nominal workspace). Each sampled point within these bounds is tested for kinematic reachability from the arm base at 9 locations (seen in yellow) including the origin frame of the site, and the 8 corners of a rectangular prism extending down from the surface origin frame.

eye calibration approach [21] using pairs of relative PTU motions and camera motions, estimated either through visual odometry or observing an AprilTag for pose. Left camera to right camera calibration, while initially provided by a stereo calibration routine, would become invalid whenever the PTU was fastened onto the lander due to the PTU stereo bar twisting slightly. Therefore, a routine was developed to exhaustively search twist angles to maximize stereo density. During sampling operations, the calibration error of the tool relative to the DEM was typically reported to be within several centimeters, which was sufficient for sampling operations.

Scoop Volume Estimation

An ancillary capability was developed to estimate sample volume within the scoop. This capability relied on an AprilTag fixed to a known location on the scoop, as seen pictured in Fig. 13, that allowed the system to recover an exact pose of the scoop within the workspace (accounting for any structural compliance and miscalibration that might bias a forward kinematics based pose estimate). By pointing the scoop's interior directly towards the stereo camera pair on the perception head, a 2.5D DEM could then be captured of the interior and compared to a CAD model of the scoop geometry; matching and subtracting the respective surfaces then produces an estimate of the volume of material within the scoop. When paired with measurements from the tool's force torque sensor, this also allowed an approximate density of the material to be deduced in testbed operations. This capability was not deployed during the field trial, as the scoop was primarily used to scrape large chunks of rock from the icy surface, rather than scoop granular material as in the lab or potentially on the surface of an icy moon.

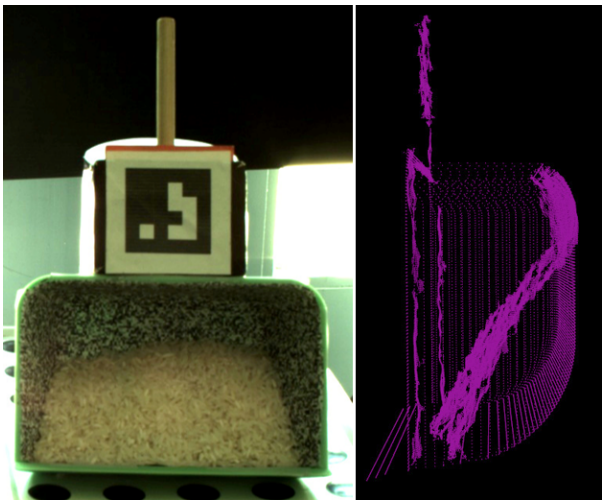

Figure 13: Left: Prototype scoop design with AprilTag and textured internal pattern that allows stereo images to determine depth of empty volume within, approx. 1/3 filled with a granular material after scooping. Right: A cross section of the stereo depth image compared against a model of the scoop geometry (positioned relative to the pose of the AprilTag), allowing the volume of the material collected to be estimated visually.

6. SAMPLING ACTIVITIES

Sampling activities were developed to meet the needs of a reference Europa Lander mission that required excavating sampling sites and collecting samples from 'targets' at depth. These were further broken down into constituent sampling behaviors that could be sequenced by a ground operator or mission planning system to achieve the ultimate objective of receipt of a sample into the theoretical lander's science instruments. Significant uncertainties in the predictions of icy moon surface properties led to potential terrain varieties being grouped into two distinct morphologies: unconsolidated-or loose, granular-and consolidated such as contiguous ice. Sampling tools and behaviors were developed to autonomously perform these activities with a scoop tool for unconsolidated materials and the ICEPIC tool for consolidated materials. For each tool, the behaviors are architected to have excavation and collection behaviors that are comprised of underlying modular behaviors on a per tool basis. At this stage of development, generic scooping and scraping behaviors exist for unconsolidated materials, with no differentiation between excavation and collection. For consolidated materials, specific excavation and collection behaviors have been developed around the ICEPIC tool.

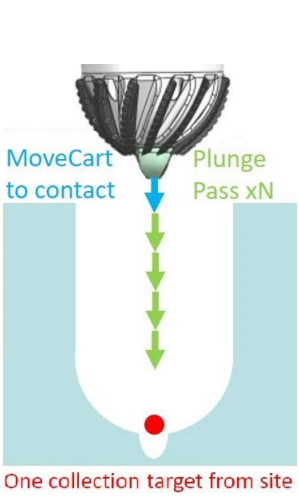

Figure 14: A "Plunge Trench" compound behavior with the ICEPIC tool in excavation mode. After an initial "Move Cartesian" to induce surface contact, the "Plunge Pass" behavior is called repeatedly until depth goal is achieved.

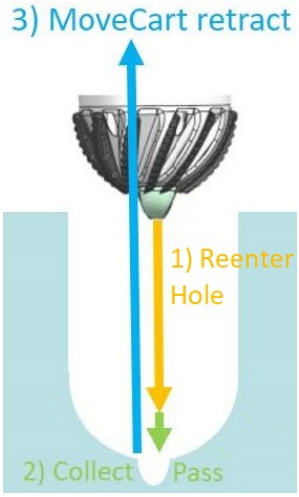

Figure 15: A "Collect" compound behavior with the ICEPIC tool in collection mode. After a "Reenter hole" behavior finds the base of previously excavated hole, "Collect Pass" acquires material and then retracts the tool.

Unconsolidated Excavation

Scooping—A generalized scooping behavior was developed to employ the scoop tool shown in Figure 5 to excavate and collect unconsolidated-or loose, granular-material. This is achieved by lifting material away from the substrate or bulk material and depositing in another location. A single scoop pass moved the tool along the sagittal plane of the robotic arm in a smooth arc, while rotating the tool to keep a constant angle of attack to the surface. Each pass was defined by its length, maximum depth, and angle of attack. To remove material in regions larger than the internal volume of the scoop, the area was divided into multiple passes, grouped into

series of passes along each layer, and multiple vertical layers. Each layer is evaluated from a target area at a given depth, and a simple granular model was used that considers the angle of repose of the material, resulting in a pyramid-like structure.

A reactive behavior was implemented to avoid large forces in the robotic arm, due to an inclusion or a hard substrate like ice. If the forces perpendicular to the surface were higher than a safety threshold, as measured by the force torque sensor on the tool wrist, the tool was retracted against the surface. The magnitude of the retraction was proportional to the violation of the maximum force target. The proportion constant was found empirically during testing as a trade-off of tool responsiveness to changes in the terrain and trajectory smoothness. A high value resulted in constant jumps as it retracted very fast. Similarly, a low reaction constant increased the time to settle as the terrain changed. Note that only forces higher than the safety margin were penalized, and the tool followed the prescribed trajectory for forces below that value. This behavior was shown to be effective during the field experiments with gravel and ice shavings, even in the presence of a hard ice substrate and a stiff robotic arm and lander system.

Scraping—A special behavior was implemented for very thin layers of loose material on an irregular hard substrate, as encountered in with moraine gravel on Matanuska Glacier. In this terrain, the scoop was unable to dig deep enough to extract significant material inside. An alternative approach of scraping inverts the scoop to press the scoop leading blade against the surface to a specified preload and move along its sagittal plane at a constant angle of attack. Unlike with scooping, this approach does not rotate the scoop to follow a smooth arc. This approach results in the scoop blade dragging along the substrate surface and pushing the unconsolidated material along the scoop's direction of motion to reveal the substrate below. The same reactive behavior as described in the scooping section was used for scraping, resulting in the scoop accommodating to the irregularity of the terrain. Figure 4 shows the result of multiple scraping passes during one of the experiments.

Consolidated Excavation

Plunge Trench—The prototypical excavation method for the ICEPIC tool was that of plunge trenching, as depicted in Fig. 14. The tool would move in joint space to come within 10cm of the perception supplied surface, and then use a move-to-contact behavior to engage the surface. A vertical force setpoint with side load nulling would then be applied along the surface normal and rate of progress regularly checked autonomously for signs of rate of penetration falling below specified levels, which could indicate having contacted a solid subsurface inclusion or clogging of tools flutes.

Early lab testing and observations of common drilling practices demonstrated the need for cutting clearing maneuvers in the behavior. This need was exasperated by the fact that the ICEPIC tool was particularly susceptible to clogging of flutes that would reduce cutting efficiency. The behavior implemented a periodic clearing at specified depth intervals and as a response to low rate of penetration. This clearing involved retracting the tool all the way out of the excavated volume to several centimeters above the surface. The behavior would then re-enter the excavated volume along its original trajectory. The periodic retractions for clearing required extra time but enabled greater excavation depths.

While this excavation approach was the most expedient to achieve desired depth, it would only yield a single point viable for collection of a sample given the cross section perfectly matches the shape of the tool. A Europa Lander mission may require the option of selecting from a set of collection targets within an excavated site. This would required increasing the access area at the base of an excavated volume.

Plunge Array— One means of increasing the area across which samples could be collected was to compound multiple plunge trenches into a laterally spaced array, as seen in Fig. 16. Subsequent plunges were placed less than one radius apart to ensure sufficient overlap of each trench such that, upon completion, a lateral motion at the base of the trench would create a continuous surface across which to choose collection sites. This approach proves effective for clearing wider regions of surface material due to predominantly relying on a plunge feed direction where the ICEPIC tool was most energetically efficient.

The plunge array behavior required modification of the lateral load nulling approach used in the single plug. This approach seeks to limit side forces induced on the tool during drilling. While this helped during a single plunge, when successive plunge sites were placed within one radius of each other, the lateral nulling would cause the software to to deflect the tool trajectory sideways towards the previous hole where there was less material to generator side loads. This was mitigated by running an initial 'predrill' plunge of several centimeters depth *without* side load nulling, to establish a new local minimum on the topography, and then resume plunge excavation with side load nulling enabled.

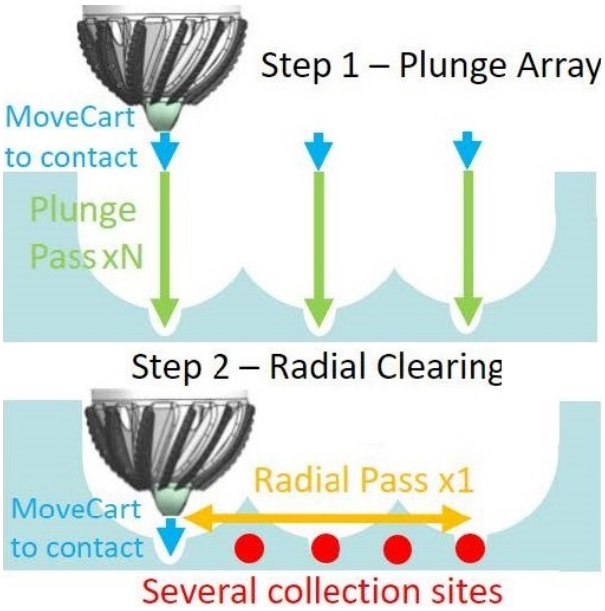

Figure 16: A "Plunge Array Trench" compound behavior. A sequence of 2-5 "Plunge Trench" behaviors are placed side by side to expose a larger subsurface region, after which a single "Radial Pass" clears a flat base to enable collection anywhere across the 1D region.

Radial Trench—An alternative method to achieving a greater viable collection area was the radial trench. This sought to leverage the purported ability of the ICEPIC tool to excavate laterally like an end mill, however, the empirical results demonstrated that material removal energy efficiency was

significantly greater when feeding along the plunge direction. The radial trench behavior also induces large side loads at the tool tip that would saturate the force torque sensor's moment axis on both robotic arms. As such, the radial trench method, seen in 17, was only employed within the laboratory environment and not qualified during the field trial deployment.

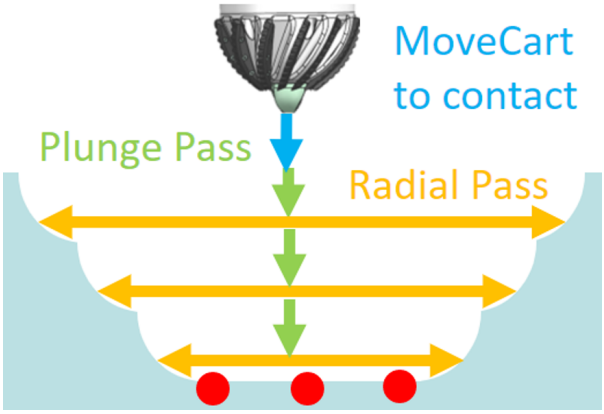

Figure 17: The "Radial Trench" behavior employed a series of alternating plunge passes and then lateral radial passes to excavate decreasing widths of material to expose a continuum of subsurface collection area. This proved less energetically efficient than a plunge array trench due to the reduced cutting efficiency of lateral motion with ICEPIC.

ICEPIC Collection

Once either sufficient material has been removed, or an operator decides to conduct a surface sample, we move on to collecting material using the cavity within the ICEPIC tool. This employs the same underlying motion primitives as excavation, such as is depicted in Fig. 15, save that the manual reconfiguration of the tool that retracts the center routing bit allows material to accumulate within the interior of the hollow tool. After a parameterized depth of penetration, the tool is retracted from the collection site, but remains spinning so as to retain the sample within it.

The arm can then sweep through joint configuration space, while avoiding self collisions, so as to bring the orifice of ICEPIC over the sample receptacle. Upon halting the tool, any sample within the cavity falls into the receptacle in order to be weighed and assessed for sufficiency. Depending on the mass collected, the mission autonomy may choose to repeat the collection at that same location, or declare sampling success. Although the method of autonomous sample transfer developed at this time relies on gravity, the ICEPIC tool and other Europa Lander collection tool prototypes are able to transfer sample out of a tool into a lander processing system via non-gravity means such as pneumatics.

ICEPIC Autonomous Responses

While the compound behaviors described above presume a nominal execution with no fault cases, interaction with tough substrates was easily capable of causing faults within the autonomous sampling system. Chief among these was the issue of spindle stall, when excess normal or lateral forces would cause the spindle actuator that drives the ICEPIC tool to either exceed current limits or fail to track velocity set points. Providing means to both autonomously engage preventative actions, and respond to the spindle faults when they happen, was the single most enabling capability in achieving fully autonomous end-to-end mission executions.

Tool stall happens when the tooling behavior exceed the limit of tool spindle motor, as seen in Fig. 18. This can happen in various levels of fault:

1. High-level fault: the tooling progress is below temporal threshold and the software faults out.
2. Mid-level fault: when the tooling motor falls behind the commanded velocity, the software faults out with velocity tracking error.
3. Low-level fault: When the motor exceeds the peak current limit for a certain duration of time, the motor controller ramps down the output current to continuous current to protect the hardware. This typically leads to a velocity tracking error as well.

Preventative actions were taken by monitoring the current sourced by the spindle actuator while maintaining a fixed velocity setpoint, and when this current begins to trend above the certain ratio of the maximum, the normal force being applied along the tool would be reduced. This served to reduce the incidence of spindle stool faults on the order of 70%, greatly increasing the speed with which the autonomous system could complete excavations and collections within both the laboratory and field test environments.

However, the remaining 30% of spindle stall faults were experienced when reduction of normal force was insufficient to prevent them. To address these lingering faults, the autonomous motion control system needed to be equipped with the means to self-clear fault conditions, retract the tool along its normal, and direct the tool to recommence the faulted behavior. During reattempts, faults would sometimes reoccur if the tool performance leading to the faults were consistent at a given site. In some cases this could lead to cycles of autonomous self-clearing and reattempts that would eventual be terminated by a high level slow progress fault. These techniques enabled all behaviors with the ICEPIC tool to execute unaided by an operator in the presence of high tool performance variability, thus allowing the system to complete the numerous end-to-end mission runs it was subjected to throughout the field campaign.

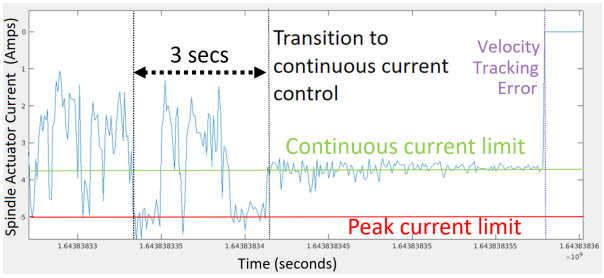

Figure 18: An example of spindle stall occurring while plunging the ICEPIC tool into an ice sample within a laboratory environment, before autonomous mitigation strategies were developed. The plot shows the current of the spindle actuator, where a sustained value above the peak limit triggers a switch from velocity control mode to current control mode, and finally a velocity tracking error causes a complete stall of the tool.

7. Field Campaign Outline

The field campaign was designed to elicit sampling performance and autonomous responses by the sampling autonomy that could not be easily generated in the lab. To that end, the team selected an accessible glacier test site that would provide variation along ice makeup, sampling tool scale geometry, and lander scale topography. Matanuska Glacier was identified as having these characteristics by local site experts, JPL science team members, and previous JPL visits to the location. While other glaciers possessing similar characteristics could be found internationally, selecting a domestic location greatly simplified logistics due to the challenges associated with 'export' of such technology. A three week campaign was planned that afforded testing at three locations on the glacier over the period. Robotic equipment and support equipment was helicopter slung to each location from a off-glacier basecamp and kept at each location for several days. The operations team conducted daily glacier treks across moraine terrain to the test locations with the aid of glacier guides.

Site Selection

The three test locations on the glacier were selected to provide increasingly complex sampling tool scale geometry, lander scale topography, presence of moraine gravel, and ice veins as the campaign went on. The three locations are referred to as site A, B, and C. Site A was generally flat (<5deg slope) with homogeneous ice. Site B had gently sloping terrain (5-10deg) with shallow scattering of moraine gravel and small ice veins. Site C had 8-12deg slope, 30-40cm step features, deeper moraine gravel, and a large ice vein.

Field Sampling Activity Plan

Arrangements of the behaviors described in Sec. 6 were selected for field execution on Matanuska Glacier as both individual behaviors, sampling activities, and end-to-end mission executions. Activities required by the reference mission were identified as 'baseline' field activities. 'Reach' activities were identified to attempt more complex capabilities given success along the baseline set. These field sampling activities are listed with goal execution counts for the field campaign in Fig. 19.

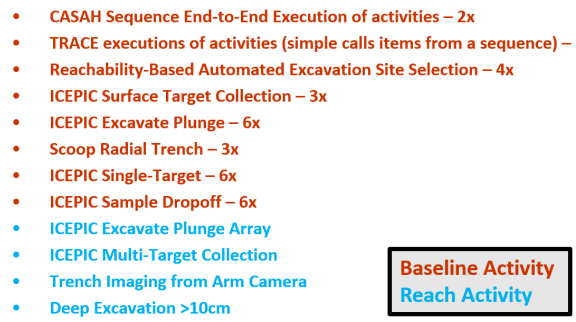

Figure 19: Activities planned for operations on the glacier. 'Baseline' activities were considered required for a reference mission, while 'Reach' were extensions of varying complexity to attempt only once baseline activities were complete.

8. RESULTS

Activity Summary

The field campaign at Matanuska Glacier was able to far exceed all the goal execution counts for baseline sampling activities and was able to attempt all reach activities. The successful executions were distributed across all three glacier sites. A summary of the executed activities is provided in Fig. 20.

Approximately half of the executions involved operator intervention with the other half executing to successful completion autonomously. Most of the interventions were addressing various integration and high level configuration issues that had not previously been identified in the lab setting, e.g. properly setting arm teachpoints on the field lander for sample drop-off and hand-offs between behaviors. A smaller subset of the interventions dealt with behavior performance that required threshold updates or software bugs that required behavior updates.

Performance Observations

A variety of observations were made around the performance of the sampling system in the glacier environment.

Lander Stability—Much like a Europa Lander mission, the performance of the field sampling system was impacted by the stability of the lander mock-up on the glacier environment. The lander was stabilized on the terrain through a high-traction belly pan and lockout articulated legs equipped with spiked feet. Throughout test days the icy substrate underneath the lander and the lander feet would melt due to environmental conditions. As the icy melted, the feet would lose purchase and the ability to react loads. The belly pan would tend to rest on a ever decreasing area of ice. To compensate for melting phenomenon, 2-5 times a day operators would adjust the position of the landing leg joints to maintain contact between feet and ice, and keep the lander under 15deg tilt. This melting phenomena is analogous to the potential sublimation of the Europan surface around and under a lander due to radiation and conductive heat transfer from the lander.

Stability of the lander with respect to sampling loads and lander articulation can be assessed against the consistency of the lander's attitude and susceptibility to slip. An observation of the campaign was that as stability decreases relative to these metrics, sampling behaviors experienced more faults. As sampling tools generated vibrations through the arm, less stable lander configurations would lead to more and more aggressive whole lander vibrations that would ultimately induce side load limit and spindle stall faults.

These vibration events and gradual loss of stability between leg resets would also induce small lateral slip that posed challenges to targeting of the sampling system. At various points during the sample chain, the tool needs to re-enter an excavated volume that has a target defined in lander frame, but physically exists in world frame. Slips beyond 1-2cm would lead to terrain collisions issues between the tool the generated tool side loads incompatible with the sampling behavior thresholds.

Sampling Behaviors—The site selection algorithm provided operators with a variety of reachable exacavtion sites and collection targets across the workspace. Fig. 21 depicts the sites that were chosen by operators at lander placement site C, with a range of orientations and surface materials across

		Date	28-Jul	29-Jul	30-Jul	31-Jul	1-Aug	3-Aug	4-Aug	5-Aug	6-Aug	8-Aug	9-Aug	10-Aug	11-Aug
		Day Type	Move/Checkout	1/3	2/3	3/3	Move/Checkout	1/3	2/3	3/3	Move/Checkout	1/4	2/4	3/4	4/4
		Site	A	A	A	A	B	B	B	B	C	C	C	C	C
		Arm	Luigi	Luigi	Luigi	Luigi	Luigi	RING	RING	RING	RING	RING	RING	RING	RING
Attempted Activities	**Totals**	**Goals**													
ICEPIC Excavate Plunge	18	6	1	2	1			1	3		1	2	2	4	1
ICEPIC Single-Target Collection	10	6	1	2	1				1		1	2		1	1
ICEPIC Sample Dropoff	12	6	1	2	3				1			2	1	1	1
ICEPIC Surface Target Collection	3	3			1								2		
Scoop Radial Trench	16	3				10	4			3			2		1
ICEPIC Excavate Plunge Array	1	Reach			1										
ICEPIC Multi-Target Collection	0	Reach													
ICEPIC CASAH End-to-End	8	2		2					1		1	2	1		1
ICEPIC TRACE End-to-End	7	1			1							3		3	
Automated Target Selection	23	4	2	2	3			1	1	3	1	5	1	3	1
Deep Excavation	2	Reach			1									1	
Trench Imaging from Arm Cam	1	Reach								1					

Figure 20: Activities that were completed during the three weeks of operations, meeting targets for all baseline, and some reach goals.

the topography so as to exercise the full capabilities of the RiNG arm and ICEPIC tool. None of the sites excavated with either the Luigi or RiNG arm encountered kinematic issues, demonstrating the efficacy of the site selection algorithm. This was of greater import for the 5-DoF Luigi arm, as the 7-DoF RiNG arm possessed no kinematic deficiencies as long as joints were kept away from singular configurations; while the Luigi arm required approach angles and excavation trajectories to be generated that complied with the Yaw-Pitch-Pitch-Pitch-Yaw joint topology. This was achieved by projecting the average local surface normal at each proposed site onto the sagittal plane of the Luigi arm shoulder, to establish the closest angle at which the tool could conduct plunge drilling operations without requiring motion in an unrealisable direction.

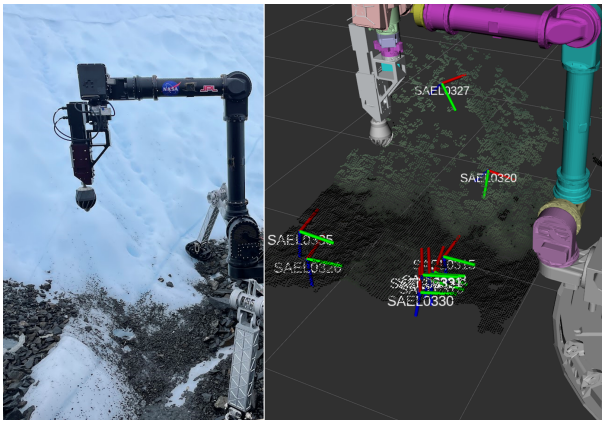

Figure 21: Left: The sampling workspace of the lander at site C, with RiNG arm in ready configuration. Right: The variety of excavation sites within the site C workspace that were proposed autonomously by the software stack, and then selected by the 'ground operators'. Site proposal involves observing operator specified keep-in and keep-out zones, reachability analyses for varying sizes of potential excavations, and overlap with other proposed sites.

Autonomous fault prevention and recovery techniques allowed the system to complete excavation and collection tasks with few operator interventions due to sampling behavior algorithm performance or hardware safety, a significant improvement from earlier laboratory and ORT test campaigns where frequent corrective action was needed. This was even true of the 27cm extended plunge excavation that was conducted on site C, as pictured in Fig. 22, that was only stopped when the geometry of the tool spindle gear housing began to interfere with the topography.

The example case where intervention was required occurred when a set of small rocks fell into the partially excavated hole. The excavation proceeded a clearing a small patch of moraine gravel from the site using the scoop scraping behavior. The rocks seen in Fig. 23 caused rapidly increasing spindle currents. As the current was increasing over the course of several seconds, operators noticed a large vibration in the robotic arm and lander and an unusual noise. At this point operators stopped progress of the autonomous sampling behavior due to concerns for hardware safety. The rapidly increasing spindle motor currents are seen in Fig. 24. This sampling anomaly was particularly interesting due to being caused by an interaction between significantly different terrain types (ice and rock) as well as illustrating a true hardware risk to the tool. This is a plausible anomaly for a future mission and should inform development of future autonomous fault protection.

Beyond the sampling behavior interactions with the environment, the autonomy stack proved capable of robust operation both with ground operator sequencing, and when connected to the TRACE mission planning autonomy stack (Fig. 10). Voluminous telemetry and screen logs were automatically collected and indexed with only the need for operators to issue start or stop commands, with contextual video feeds placed strategically about the workspace that were post-processed into varying levels of compression overnight via automated pipelines. Alongside this rapid turnaround logging and post-processing infrastructure, on several days at site B the operations team established a direct video stream of the operator interface and context videos back to the Jet

Figure 22: Left: The lander conducting an extended plunge excavation at site C, with the ICEPIC tool pictured deep into the ice on bottom left. Middle: The ICEPIC tool exiting the plunge trench. Right: Measurement of the extended plunge trench which netted 27cm of depth under the original surface.

Figure 23: Top: After images of an excavation trench at site C where several rocks fell into the hole during excavation necessitating a manual abort. Bottom: The offending rocks measured for scale.

Figure 24: Top: The tool forces in the Y (lateral) and Z (axial) directions during excavation when rocks entered the trench. Bottom: The current drawn by the ICEPIC spindle motor, seen to increase significantly. Operators aborted the test due to large vibrations observed on the lander concurrent with the high spindle current.

Propulsion Laboratory for interested parties to follow their progress.

The autonomy stack's kinematics and manipulation capabilities also proved to be robust to varied actuator topologies, as the RiNG arm was only delivered in full form one day before departure to Matanuska, and yet was operational on the first day. Scooping and scraping behaviors were also developed on a third arm not deployed to the field trial named SaMY, of a similar 5-DoF YPPPY configuration to Luigi but with significant differences in joint spacing and configuration. The sagittal parameterization of the YPPPY reachable workspace allowed behaviors developed on the SaMY arm to be directly transferable to both the Luigi and RiNG arm, with only two updated parameters to define the sagittal plane distance and maximum reach.

9. LESSONS LEARNED

A list of lessons learned was generated by the team to inform future sampling autonomy development efforts and field campaigns.

- Operational Readiness Tests are key. One was conducted at Jet Propulsion Laboratory's 'Mars Yard' and in the field before heading to the glacier which significantly improved our operational efficiency.
- Bring more sampling tools to the field to be used with hand tools in order to explore effects of natural features on tool performance and explore new tool operation modes.
- Bring better site characterization tools such as hardness tester, microscope.
- Target sites with meter-scale relief to further challenge perception and autonomy.
- Develop a remote design sim synced up with the field campaign. Let the field team act as the lander autonomy, and allow JPL team to discuss and plan out alternative sampling plans.
- Label all your cables and what ports they go into.
- Carry multiple sets of many tools to allow for parallelization of hardware support tasks.
- Make as of your equipment rainproof as possible.
- Canopies and tent walls were key for team efficiency.
- Grow awareness of the jobs of your peers so you can form your activities around theirs.
- Bring a handheld kinematic model of the arm to the field. Bring a white board to draw out plans.
- Spend as much time as possible on setting up good video capture. Test capture strategies before hand.
- Make autonomy teachpoints highly editable by field operator in order to adapt to new terrain and activities.
- The functional sample behaviors worked very well, but there is plenty of room for speed up, and further robustness that leverages the sensing and force control.
- Pecking type of behavior on ICEPIC seems to induce faster excavation rates. The dynamic contact with the ice removes material more quickly.
- Scooping thin layers of hard, unconsolidated, large-grain materials is difficult. Scraping appears to be more robust and time efficient. A scoop with points like a backhoe would allow for better penetration and leverage when scraping.
- Hard rocks falling into excavation holes present hardware safety risks. Anomalies like this should be autonomously detected through force torque and spindle current sensing.
- The high likelihood of decimeter-scale lander slip requires frequent terrain targeting updates that account for the changing global kinematic pose of the lander.
- The test sites typically had enough visual texture for stereo local block matching to produce a dense DEM, but semi-global matching was required for texture-poor ice.

10. FUTURE WORK

Given the uncertainty in the Europan surface, sampling autonomy should make use of in-situ learnings to improve performance as a mission goes on. While several techniques for extrapolating from historical excavation data to potential future sample sites were conceptualized, they were not integrated with the full autonomy system that was demonstrated in the field trial. The data from the in-situ excavations on Matanuska Glacier indicated a highly bi-modal distribution of material properties, where unconsolidated or granular surface material was well suited to scooping or sweeping aside, and consolidated ice required aggressive removal with an active tool. This may motivate a surface representation that captures a binary distinction between these two regions, perhaps as two overlayed DEMs capturing one granular surface and one consolidated surface, without need for significant terramechanical fidelity beyond that distinction. This could then inform tool selection, with clear delineation in the case of being equipped with a scoop and active rotary tool.

Despite the design intention of the ICEPIC tool to be agnostic to approach angle in terms of excavation energy efficiency, testing in lab and in the field trial proved otherwise. This constrained the compound trajectories that could be realized, such that only those composed of sequential plunge passes proved effective, despite a number of other approaches, in particular the radial trench, being considered advantageous. Other tools are currently in development that should enhance the lateral energy efficiency of excavation, and future autonomy development efforts may be able to leverage this removal of angle of attack dependence with more advanced excavation geometries.

The addition of a camera within the tool electronics housing allowed the robotic arm to be used to capture a 'selfie' of the lander, but the full benefits of having a highly (locally) mobile field of view camera were not realized within the autonomy. The RealSense D435i mounted on the arm could have allowed point clouds to be generated from a range of angles about a given excavation site within the workspace, developing a high fidelity model of the status of excavation, along with high resolution RGB images of the substrate being interacted with. This data could also be used to improve overall DEM coverage in regions where terrain or the lander body occlude the mast-mounted cameras. Future endeavors may seek to make better use of these arm-mounted depth mapping capabilities to improve surface models for sampling.

As most of the excavation and sampling behaviors were developed on the 5-DoF Luigi arm, they were designed with kinematic constraints in mind that limited the space of tool motions that could be undertaken. With the deployment of the 7-DoF RiNG arm occurring during the field trial, these behaviors may be extended to remove some of the geometric constraints placed on them to ensure reachability with a 5-DoF system. This may afford significant reduction in sensitivity to orientation of the topography, as a surface normal that was significantly outside the sagittal plane of the YPPPY Luigi arm could not be engaged with an orthogonal tool angle. While a switch to an excavation tool less reliant than ICEPIC on a plunge approach for energy efficiency would mitigate some of the approach angle problems on relatively even terrain, a fully controllable tool orientation would enable more advanced techniques such as drilling into vertical ice walls.

ACKNOWLEDGMENT

The research described in this paper was carried out at the Jet Propulsion Laboratory, California Institute of Technology, under a contract with the National Aeronautics and Space Administration. Government sponsorship acknowledged.

The authors wish to thank Daniel Balentine, Justin Koch, Avak Archanian, Kenneth Hurst, Jose Uribe, Kevin Hand, Ken Hurst, Lori Shiraishi, Marissa Cameron, Roland Brockers, and James Round for their valuable support in the field during the Europa Lander Field Sampling Campaign (ELFS Camp). The three weeks of increasingly challenging tests relied on their technical and logistical support to enable a

successful activity. Particular appreciation goes to author Matt Gildner who demonstrated exceptional organizational skills to bring together the many elements of the successful venture. Thanks also goes to the following individuals who contributed to the development of the field lander hardware: Nikola Georgiev, Torkom Pailevanian, Katherine Tighe, Hovhannes Melikyan, Eric Ambrose, Eleni Comstock, Minna He, Aaron Yazzie, Krista Round, Rui de Gouvea Pinto, and Heidy Kelman. The field trial team also greatly appreciated the efforts of the MICA guides who navigated us safely across Matanuska Glacier each day of operations, despite tricky and ever-changing terrain.

REFERENCES

[1] P. Cassen, R. T. Reynolds, and S. Peale, "Is there liquid water on europa?" *Geophysical Research Letters*, vol. 6, no. 9, pp. 731–734, 1979.

[2] S. W. Squyres, R. T. Reynolds, P. M. Cassen, and S. J. Peale, "Liquid water and active resurfacing on europa," *Nature*, vol. 301, no. 5897, pp. 225–226, 1983.

[3] L. Roth, J. Saur, K. D. Retherford, *et al.*, "Transient water vapor at europa's south pole," *science*, vol. 343, no. 6167, pp. 171–174, 2014.

[4] W. B. Sparks, K. Hand, M. McGrath, E. Bergeron, M. Cracraft, and S. Deustua, "Probing for evidence of plumes on europa with hst/stis," *The Astrophysical Journal*, vol. 829, no. 2, p. 121, 2016.

[5] C. J. Hansen, L. Esposito, A. Stewart, *et al.*, "Enceladus' water vapor plume," *Science*, vol. 311, no. 5766, pp. 1422–1425, 2006.

[6] T. Nordheim, K. Hand, and C. Paranicas, "Preservation of potential biosignatures in the shallow subsurface of europa," *Nature Astronomy*, vol. 2, no. 8, pp. 673–679, 2018.

[7] E. Costello, C. B. Phillips, P. Lucey, and R. Ghent, "Impact gardening on europa and repercussions for possible biosignatures," *Nature Astronomy*, vol. 5, no. 9, pp. 951–956, 2021.

[8] R. Gershman, E. Nilsen, and R. Oberto, "Europa lander," *Acta Astronautica*, vol. 52, no. 2-6, pp. 253–258, 2003.

[9] J. Dooley, "Mission concept for a Europa Lander," in *2018 IEEE Aerospace Conference*, 2018, pp. 1–10.

[10] J. Bowkett, J. Nash, D. I. Kim, *et al.*, "Functional autonomy challenges in sampling for an europa lander mission," in *2021 IEEE Aerospace Conference*, IEEE, 2021, pp. 1–8.

[11] S. Chien, J.-P. de la Croix, J. Russino, *et al.*, "Onboard scheduling and execution to address uncertainty for a planetary lander,"

[12] S. Y. Kim, T.-W. Grace, A. Dhanushkodi, S. Laubach, K. Roffo, and G. Reeves, "Ground-in-the-loop mission concept study for europa lander using modeling and simulation," in *2023 IEEE Aerospace Conference*, IEEE, 2023, pp. 1–8.

[13] E. Olson, "Apriltag: A robust and flexible visual fiducial system," in *2011 IEEE international conference on robotics and automation*, IEEE, 2011, pp. 3400–3407.

[14] A. Jain, "Darts-multibody modeling, simulation and analysis software," in *European Congress on Computational Methods in Applied Sciences and Engineering*, Springer, 2019, pp. 433–441.

[15] K. Museth, "Vdb: High-resolution sparse volumes with dynamic topology," *ACM transactions on graphics (TOG)*, vol. 32, no. 3, pp. 1–22, 2013.

[16] J. Pan, S. Chitta, and D. Manocha, "Fcl: A general purpose library for collision and proximity queries," in *2012 IEEE International Conference on Robotics and Automation*, IEEE, 2012, pp. 3859–3866.

[17] G. H. Peters, W. Abbey, G. H. Bearman, *et al.*, "Mojave mars simulant—characterization of a new geologic mars analog," *Icarus*, vol. 197, no. 2, pp. 470–479, 2008.

[18] J.-P. de la Croix and G. Lim, "Event-driven modeling and execution of robotic activities and contingencies in the europa lander mission concept using bpmn," 2020.

[19] K. Edelberg, P. Backes, J. Biesiadecki, *et al.*, "Software system for the Mars 2020 mission sampling and caching testbeds," in *2018 IEEE Aerospace Conference*, 2018, pp. 1–11.

[20] A. Brinkman, J. Morris, I. Chen, N. Sheikh, and P. Warren, "Fastcat: An open-source library for composable ethercat control systems," in *2021 IEEE Aerospace Conference (50100)*, IEEE, 2021, pp. 1–8.

[21] K. Daniilidis, "Hand-eye calibration using dual quaternions," *The International Journal of Robotics Research*, vol. 18, no. 3, pp. 286–298, 1999.